ISSN 2663-1563 Vol. 6, Issue 2: 51-64, DOI: 10.25236/AJAGE.2024.060210

Joint position method of coal mines methane extraction borehole trajectory by fusing micro-seismic signal and MWD

Tao Wang[1,a], Xuelian Dong[2,*], Lili Yan[1,b], Lusi Chen[2,d], Ziwei Tian[3,e], Jingwu Zhou[4,f]

[1]*Safety Technology Centre, Sichuan Coal Mine Safety Administration, Chengdu, China*
[2]*State Key Laboratory of Oil and Gas Reservoir Geology and Exploitation, Chengdu University of Technology, Chengdu, China*
[3]*Sichuan Hengsheng Shengrui Survey and Design Co., LTD, Chengdu, China*
[4]*CCDC Drilling and Production Engineering Technology Research Institute, Guanghan, China*
[a]*623453316@qq.com,* [b]*1205338533@qq.com,* [c]*515256066@qq.com,* [d]*305311961@qq.com,* [e]*56253205@qq.com,* [f]*486807372@qq.com*
[*]*Corresponding author*

Abstract: *Drilling hole wellbore trajectory measurement is important to coal mine gas management. Current trajectory measurement technology is magnetic surveys, which adopt three-axis accelerometers (inclinometers) and magnetometers to calculate the inclination and azimuth. However, this method is easy to be affected by magnetic minerals in coal mine. This paper proposed joint position method of drilling hole using micro-seismic events of drill breaking rock and MWD (Measure While Drilling) data. This paper establishes propagation model of micro-seismic signals in rock fragmentation. Micro-seismic events pick method adopts STA/LTA (Short Term Average/Long Term Average) and AIC (Akaike Information Criterion). Micro-seismic inversion position adopts newton iteration method. Location error of micro-seismic position method is analysed influence by P-wave velocity, SNR (Signal-to-Noise Ratio), sampling frequency in horizontal and vertical direction. Trajectory calculation method using MWD data adopt Average Angle Method and Minimum Curvature Method. Hole bottom location error of two trajectory calculation methods is analysed in horizontal and vertical direction. Based on error analysis of micro-seismic location method and hole trajectory calculation method, this paper proposed two new joint location methods using Kalman filtering and weight method. According to simulate results, the precision of weight method data fusion method is better than Kalman filter method in the all direction. Ideally, the positioning accuracy of the bottom of the drilled hole can be controlled within 1m, whose depth of drilling hole is about 500m. According simulate results, proposed method can effectively improve the positioning accuracy of borehole bottom. Research results in this paper provide a theoretical reference for the boreholes trajectory measurement and calculation for coal mines.*

Keywords: *Coal mines; gas extraction borehole; trajectory measurement; data fusion; Kalman filtering; weight method*

1. Introduction

Gas extraction is an important method to solve coal mine gas disasters, utilize coalbed methane (CBM) resources and reduce greenhouse gas emissions [1]. Underground borehole extraction is main method of CBM extraction in active coal mines [2]. Trajectory of boreholes is one of the most important evaluation indexes of coal seam extraction efficiency and disaster management. Accurate measurement of borehole trajectory is significant to disaster management and resource utilization for coal mine methane [3].

Current coal mines methane extraction borehole trajectory measurement adopts triaxial accelerometer and triaxial fluxgate to obtain gravity and geomagnetic components in three orthogonal coordinates. According to gravity and geomagnetic components, inclination and azimuth of measurement point can be calculated. Trajectory of borehole can be obtained by a series measurement point of inclination and azimuth. Widely used calculation model of borehole trajectory are Average angle method and Minimum curvature method. The minimum curvature method is the most widely used for computing the coordinate deliverables of directional surveys in oil and gas drilling engineering [4]. The Average angle method is

ISSN 2663-1563 Vol. 6, Issue 2: 51-64, DOI: 10.25236/AJAGE.2024.060210

widely used in methane extraction borehole trajectory and coordinate calculation in coal mines [3].

Acceleration sensors are more accurate than fluxgates. Measurement accuracy of borehole trajectory is inconsistent in the north east and vertical direction [5]. The fluxgates are more susceptible to the influence of magnetic minerals in the formation [6]. Therefore, it is necessary to propose a novel trajectory calculation method. When drill bit contacts the bottom, the process of bit breaking rock will generate vibration signals [7]. These signals can be used to location coordinate of borehole bottom by micro-seismic detector observation array [8].

Based on the above ideas, this paper proposes a novel joint position method of coal mines methane extraction borehole trajectory by fusing micro-seismic information and MWD data. First, this paper establishes propagation model of micro-seismic signals in rock fragmentation. Micro-seismic events pick method adopts STA/LTA (Short Term Average/Long Term Average) and AIC (Akaike Information Criterion). Location errors of micro-seismic position method are analyzed influence by P-wave velocity, SNR (Signal-to-Noise Ratio), sampling frequency in horizontal and vertical direction. Trajectory calculation method using MWD data adopt Average Angle Method and Minimum Curvature Method. Hole bottom location errors of two trajectory calculation methods are analyzed in horizontal and vertical direction. Based on error analysis of micro-seismic location method and hole trajectory calculation method, this paper proposed two new joint location methods using Kalman filtering and weight method. Research results in this paper provide a theoretical reference for the boreholes trajectory measurement and calculation for coal mines.

2. Simulation of micro-seismic propagation characteristic

Micro-seismic monitoring technology, which detects elastic waves generated by rock breaking or fracturing, has been shown as an important tool to monitor mining activity [9]. Micro-seismic source usually is uncontrollable passive source of rock breakage [10]. However, signal of drill bit breaking rock is also another important micro-seismic source. This type of signal can control starting and ending time manually. Comparing with the micro-seismic signal of rock breaking, drill breaking rock signal is a deterministic signal. It is easy to identify bit breaking rock signals. This is benefit for the boreholes bottom location using bit breaking rock micro-seismic signals.

Numerical simulation of micro-seismic wave propagation provides data for hole bottom location. At present, there are two kinds of numerical simulation methods for micro-seismic propagation [11], which are Ray tracing method and wave equation method [12]. Ray tracing method ignores the influence of micro-seismic wave frequency and the arrival by non-geometric paths, which makes it impossible for most of the numerical simulation to meet the needs of the actual micro-seismic problems [11]. The following parties of this section adopt ray tracing method to simulate the propagation path of micro-seismic wave.

2.1. Simulation model

2.1.1. Model of micro-seismic signal attenuation

Micro-seismic forward modeling is the most effective means to understand characteristic of signal propagation process. There are two mainly method to obtain synthetic micro-seismic data. One is numerical method based on wave propagation equation, solved by finite-difference (FD) method [11]. Another is ray tracing method based on Snell's low, Huygens principle and Fermat's principle, including the curving ray tracing method [12], shooting method [13] and wave-front reconstruction [14].

Micro-seismic signals of bit breaking rock are attenuated when it propagates through the formation. The strength of the signal that detectors received are much lower than of original strength. The attenuation of micro-seismic waves is an extremely complex process and influenced by many factors such as density of the formation, frequency of the micro-seismic wave, temperature of the formation, pressure of the formation and so on[8]. In order to quantitatively evaluate the above influence factors, the model of quality factor Q is proposed. The formula of micro-seismic amplitude attenuation can be expressed as [15]

$$A(f,t) = A_0(f,t_0)e^{-\frac{f\pi\Delta t}{Q}} \tag{1}$$

where $A_0(f,t_0)$ is amplitude spectrum of source wavelet, Δt is travel time from micro-seismic hypocenter to the detectors, $A(f,t)$ is amplitude spectrum of received signal. In this paper, the source

ISSN 2663-1563 Vol. 6, Issue 2: 51-64, DOI: 10.25236/AJAGE.2024.060210

wavelet adopted minimum phase ricker wavelet[16].

According to the attenuation model of micro-seismic signal, amplitude of received signal is related to travel time from micro-seismic hypocenter to the detectors and distance of the propagation path. For sources of the same amplitude, the longer the propagation distance, the weaker the received signals.

2.1.2. Ray tracing method

To obtain traveling time from micro-seismic hypocenter to the detectors using the simulated micro-seismic waveform, we need real propagation path between the source and the received. Numerical simulation of wave propagation equation can describe propagation characteristic of micro-seismic wave in the formation. However, cost of the simulation of the wave propagation equation is extremely high. Propagation path of micro-seismic is not easy to identify for micro-seismic field simulation. Ray theory, a high-frequency approximation, is widely used to model elastic wave field[17]. It can obtain acceptable result with an affordable simulation time.

There are two simulation methods for ray theory, which are trial shooting method and curving bending method[18]. In order to measure coordinates of detectors conveniently, this paper adopted curving bending method to calculate the propagation path from borehole bottom and detectors. The curving bending method fixes the hole bottom and detectors and bends the ray trajectory connecting the two points to satisfy Fermat's principle.

Fermat's principle states that travel time t along a ray trajectory passing from detectors $\boldsymbol{Y}$ to $\boldsymbol{X}$ is stationary with respect to parameters governing the 3D shape of trajectory. In geological model, those parameters are the coordinated of transmission points $x(k)$ (k=1,…,K-1, as $x(0) = X$ and $x(K)=Y$ are fixed). With those preliminaries, the travel time t is formula as equation:

$$t = t(\boldsymbol{X};\boldsymbol{Y}) = \sum_{k=1}^{K} t^{(k)} = \sum_{k=1}^{K} \frac{d^{(k)}}{g^{(k)}} \tag{2}$$

where

$$d^{(k)} = \sqrt{[x^{(k)} - x^{(k-1)}] \bullet [x^{(k)} - x^{(k-1)}]} \tag{3}$$

and

$$g^{(k)} = \left|\boldsymbol{g}^{(k)}\right| \tag{4}$$

are the group velocities.

Fermat's principle requires

$$\frac{\partial t}{\partial t_j^{(k)}} = 0, (j = 1,2,3; k = 1, \dots, K-1) \tag{5}$$

2.1.3. Signal-to-Noise Ratio

The micro-seismic signals collected by the detectors are mixed with a lot of noise in a real mining environment. These noises include thermal noise of the circuit system, machine activity noise and so on. In order to simulate more realistic the micro-seismic signal of the drill bit breaking rock, we add some noise to the simulated micro-seismic signal. This paper adopted Gaussian noise to simulate actual downhole noise environment based on given SNR.

2.2. Micro-seismic location method

2.2.1. Time Difference of Arrival Location Method

At present, micro-seismic location methods mainly include arrival-time-different location method, Grid search method, Energy method and so on. There are many factors that can affect location accuracy and stability[10]. In general, a good observation system, accurate arrival time and reasonable location method can effectively improve micro-seismic positioning accuracy.

The time different of arrival location method is one of the most widely used methods in the micro-seismic location [9], such as the Geiger's method[19], the Inglada's method[20], the Thurber method[21], the Powell method[22], the genetic algorithm[23], the simplex method[24], the particle swarm method[25], and so on. The time different of arrival location method is to establish and solve multiple quadratic equation system, which include coordinates of sensors and arrival time of primary wave. The arrival time is a key to the positioning accuracy because of weak and low signal-to-noise ratios (SNR)

ISSN 2663-1563 Vol. 6, Issue 2: 51-64, DOI: 10.25236/AJAGE.2024.060210

micro-seismic signals[9].

Assume arrive time of P-wave to each sensor is T_i ($i = 1, 2, \ldots, n$), and then calculated time of P-wave to each detectors are:

$$\hat{T}_i = \frac{l_i}{c} + T_0 \tag{6}$$

From the distance formula of two points in the same formation, it can be expressed:

$$l_i = \sqrt{(x_i - x_0)^2 + (y_i - y_0)^2 + (z_i - z_0)^2} \tag{7}$$

The arrival time T_i, P-wave velocity c and coordinate of detectors (x_i, y_i, z_i) are known, however, the coordinate of detectors (x_o, y_o, z_o) and time of source generation are not given.

According to the time different between arrival signals, the objective function can be derived:

$$\min f = \sum_{i=1}^{n} \left(\hat{T}_i - T_i\right)^2 \tag{8}$$

Above equation is a nonlinear optimization problem. The value of (x_o, y_o, z_o) and T_0 can be obtained by solving its least squares solution. Wave velocity can be assumed to be consistent at the scale of a single coal seam in a mining area. Under the ideal condition of single velocity model, when location calculation is absolutely accurate, the calculated time $\hat{T}_i$ and the arrival time T_i should be equal.

$f(x)$ a first-order Taylor multinomial expanded at x_0 can be expressed as:

$$f(x) = f(x_0) + f(x - x_0) f'(x_0) \tag{9}$$

Then

$$x = x_0 - \frac{f(x_0)}{f'(x_0)} \tag{10}$$

Newton-lafson method produces an order in an iteration:

$$x_{n+1} = x_n - \frac{f(x_n)}{f'(x_n)} \tag{11}$$

The minimum value of the objective function can be obtained by iterating the above formula repeatedly.

2.2.2. Event pickup method

There are massive methods to pick up the arrival time of micro-seismic signal, such as STA/LTA picker and AR-AIC model[26], AIC picker[27, 28], EMD-based picker[29, 30], Cross correlation technique[31], Waveform fractal based algorithm[32], AMPA algorithm[33], Wavelet transform based algorithms[34], Neural networks based algorithms[35]. Although there are so many event pickup algorithms, the STA/LTA picker and AIC picker are the most widely used approaches in the micro-seismic event pickup.

The short-time-average/long-time-average (STA/LTA) trigger is usually used in weak-motion applications that try to record as many micro-seismic events as possible. It is nearly a standard trigger algorithm in many real time processing software packages of the weak-motion seismic networks[36]. The calculation formula is shown as follow:

$$R = \frac{STA}{LTA} = \frac{\sum_{i=1}^{N} X(i)/N}{\sum_{j=1}^{M} Y(j)/M} \tag{12}$$

Where, $x(i)$ indicates data recorded in a short window, $i = 1, 2, \ldots, N$; $y(i)$ indicates data recorded in a long window, $i = 1, 2, \ldots, M$; M and N are number of samples of long window and short window respectively.

STA/LTA algorithm can only pick up the approximate time of the P-wave arrival based on given threshold value. The picked arrival time varied as threshold value. STA/LTA algorithm can only pick up the approximate time of micro-seismic event. In order to pick more accurate arriving time of micro-seismic event, AR-Akaike information criterion (AIC) is adopted. AR-AIC algorithm can be expressed as follows[26]:

$$AIC(k) = kln\{VAR(CF(X[1,k]))\} + (N - k - 1)ln\{VAR(CF(X[k+1,N]))\} \tag{13}$$

Where, $X[1,k]$ is micro-seismic waveform data, k is all micro-seismic signal sampling points in the time window, N is the length of the micro-seismic signal, VAR is variance function, CF is characteristic

ISSN 2663-1563 Vol. 6, Issue 2: 51-64, DOI: 10.25236/AJAGE.2024.060210

function. VAR-AIC algorithm has the advantages of simple calculation and high picking accuracy[37].

2.3. Location error factor analysis

The accuracy of micro-seismic location method is affected by many factors. In this section, we will discuss influencing factors of micro-seismic location accuracy. Monte Carlo simulation method is adopted to simulate the location process. Probability distribution of location error is calculated.

2.3.1. Event pickup method

A probability evaluation method for micro-seismic location errors was proposed in this paper. Firstly, determine the hole bottom position and detectors position. Secondly, according to hole bottom position and detectors position, determine the propagation path of micro-seismic signal. Thirdly, micro-seismic signal waveform is synthesized considering noise and attenuation. Fourthly, arriving time are picked by STA/LTA and AR-AIC method. Fifthly, the position of borehole bottom is calculated by Newton iteration method and location error in X Y Z direction are calculated. Finally, statistical parameters of location error are calculated using unimodal and bimodal Gaussian fitting[38].

The detailed procedure is as presented in the Figure 1:

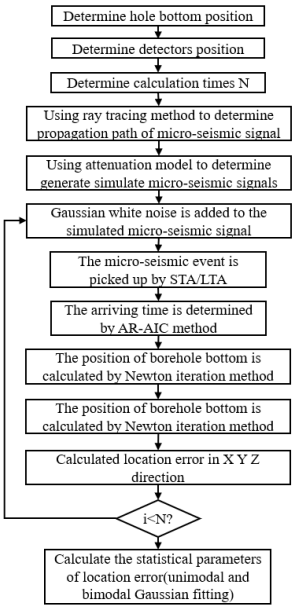

Figure 1: Micro-seismic signal location error analysis process.

2.3.2. Observation system and position of hole bottom

Observation system consists of 12 detectors. Because the coal seam is generally horizontal, these detectors distribute on an approximate horizontal plane. The coordinates of observation system detectors are presented in the Table 1:

Table 1: The detectors coordinate of observation system.

No.	X(m)	Y(m)	Z(m)
1	-700	0	100
2	-300	0	10
3	-100	0	0
4	0	0	0
5	330	0	-30
6	800	0	-50
7	-600	960	40
8	-500	1000	40
9	-400	1100	0
10	0	1000	0
11	320	1000	-60
12	600	1100	-100

The true coordinate of hole bottom is (8, 500, 0). The P-wave velocity is 2200 m/s, SNR value is -

ISSN 2663-1563 Vol. 6, Issue 2: 51-64, DOI: 10.25236/AJAGE.2024.060210

4dB, the quality value is 10, the sampling frequency is 2000Hz, simulation time is 0.6s. The synthesized 12-channel micro-seismic waveform is shown in the Figure 2.

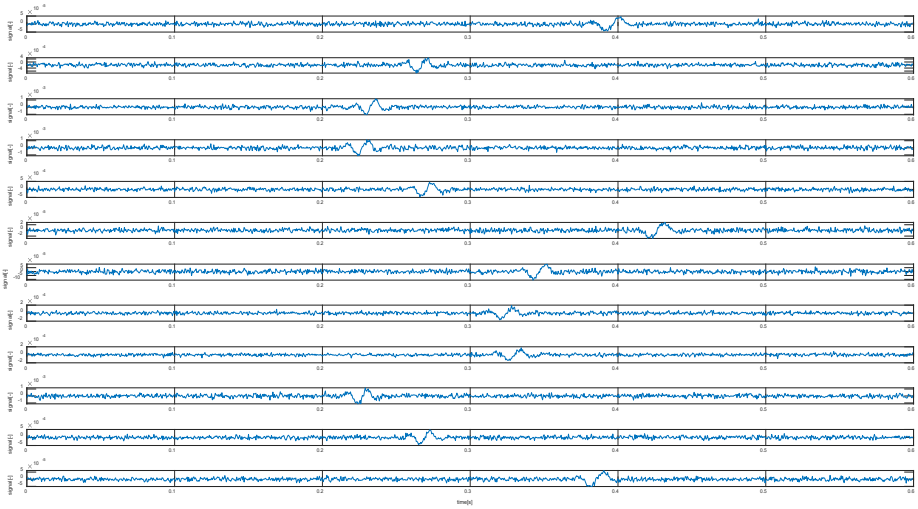

Figure 2: Synthetic micro-seismic waveform of detectors.

According to simulated micro-seismic waveform, arrival time of micro-seismic signals of each detector are different. The added noise in micro-seismic signals will result in an error at arrival time picking. STA/LTA method can effective pickup arriving time of the micro-seismic signal. The AR-AIC method has higher picking accuracy comparing with STA/LTA method in the Figure 3.

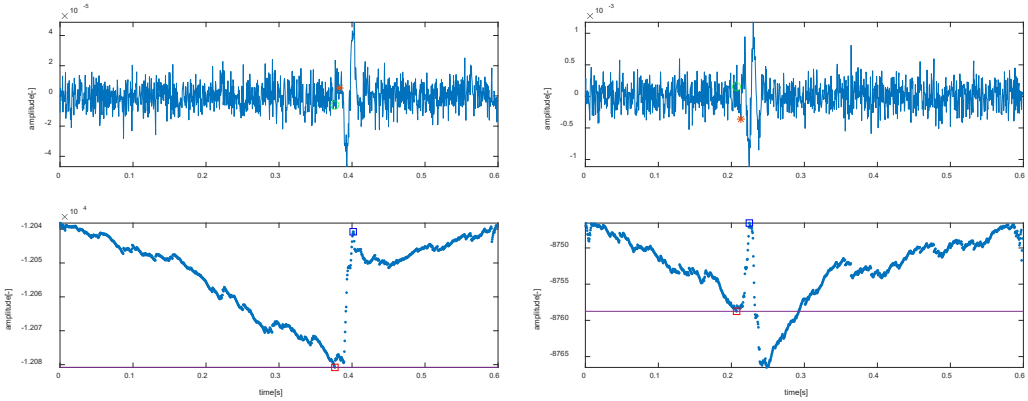

Figure 3: Event picking of detectors synthesis waveform (partial).

2.3.3. Influence of P-wave velocity

P-wave velocity of micro-seismic wave varies with rock lithology. The wave velocity of sedimentary rocks range from 1500 m/s to 6000 m/s. P-wave velocity of coal rock is affected by effective stress, pore pressure and so on[39]. According to laboratory studies results, P-wave velocity of coal rock is varied from 1000 m/s to 2500 m/s. In this study, we set P-wave velocity from 1800m/s to 2400m/s with 200 m/s step. SNR of simulated micro-seismic signals is 10dB. Quality factor is 10. Sampling frequency is 1000 Hz. Simulate time is 2s. Location error probability density distribution is presented in the Figure 4.

ISSN 2663-1563 Vol. 6, Issue 2: 51-64, DOI: 10.25236/AJAGE.2024.060210

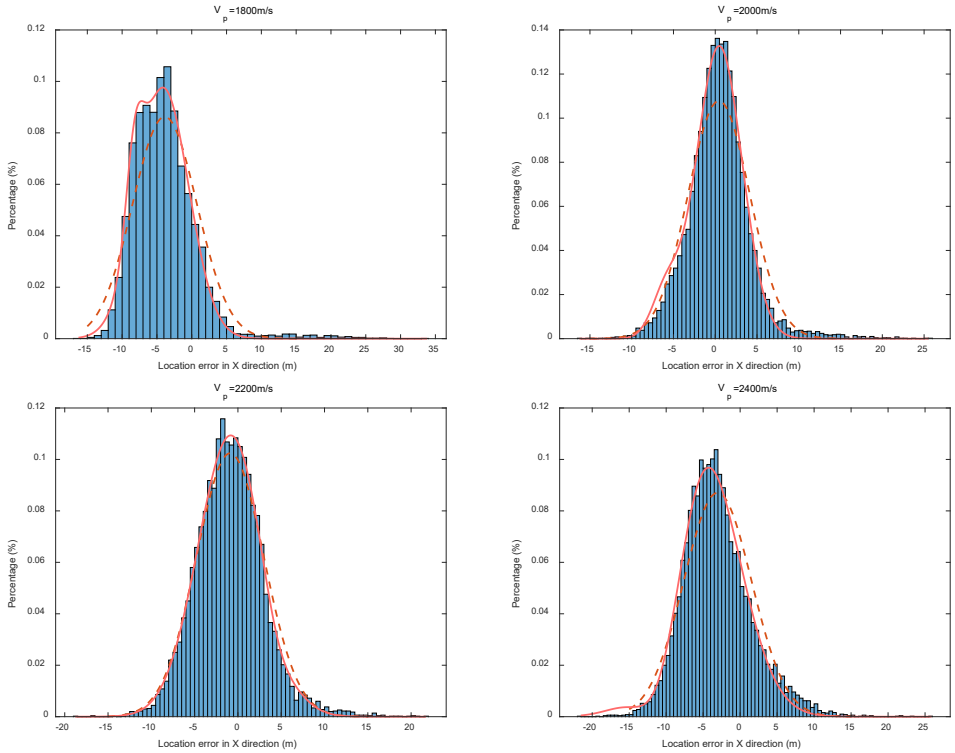

Figure 4: Location error probability density distribution with varied P-wave velocity.

Location error probability density distribution in X direction is approximate normal distribution. However, bimodal normal distribution agrees better with the simulation data. According to expectation and variance pattern, smaller P-wave velocity (1800 m/s) leads to increase location error. However, as the P-wave velocity increases, the expectation of location error increases. There is a best P-wave velocity with the least location error. According to the Table 2, the best P-wave velocity value is between 2000 m/s to 2200 m/s.

Table 2: Gaussian fitting results for location errors with varied P-wave velocity.

Velocity (m/s)	Bimodal normal distribution				Unimodal normal distribution	
	Peak1		Peak2		Expectation	Variance
	Expectation	Variance	Expectation	Variance		
1800	-4.094	5.185	-8.196	1.757	-3.87896	4.6266
2000	0.4724	3.88	-5.88	2.367	0.439143	3.70045
2200	-0.8132	5.367	4.327	2.386	-0.899149	3.89595
2400	-5.268	7.053	-10.11	4.381	-3.042	4.58425

2.3.4. SNR

The SNR of the simulated micro-seismic signal affect accuracy of the arrival time. In this section, the effect of signal-to-noise ratio is analyzed by Monte Carlo simulation. In the simulated model, SNR is set to 10 dB, 7 dB, 3 dB and 0 dB respectively. P wave velocity is 2500 m/s, quality factor is 10, sampling frequency is 2000 Hz, simulation time is 10000.

Table 3: Gaussian fitting results for location errors with varied SNR.

SNR (dB)	Bimodal normal distribution				Unimodal normal distribution	
	Peak1		Peak2		Expectation	Variance
	Expectation	Variance	Expectation	Variance		
10	-5.084	3.003	-1.554	5.047	-2.76219	3.53893
7	-2.274	4.812	3.377	4.436	-0.84995	4.11664
3	2.171	8.879	8.714	5.261	0.790929	5.89876
0	3.159	4.654	-0.01599	13.25	0.919607	17.9255

According to simulated results, micro-seismic location error satisfies the normal distribution function

ISSN 2663-1563 Vol. 6, Issue 2: 51-64, DOI: 10.25236/AJAGE.2024.060210

when SNR is greater than 3dB. When SNR value is 0dB, location error varied range increase. Higher SNR is benefit to reduce the micro-seismic location error. According to parameters of fitted probability density function in the Table 3, SNR fewer effect on expectation. However, variance of fitted normal density function increase as SNR increased.

2.3.5. Sampling frequency

The sampling frequency of micro-seismic monitoring system are different between each manufacturer. The sampling frequency range of mainstream equipment is from 1000 Hz to 6000 Hz[40]. In this section, sampling frequency are set to 1500 Hz, 2000 Hz, 2500 Hz and 3000 Hz respectively. According to probability density function fitted results, greater sampling frequency has greater location error variance. It indicated that greater sampling frequency reduce location error range, however, the effect is little weak. Fitted results of the bimodal and unimodal normal distributions, expectation and variance in the Table 4 become less different with increasing sampling frequency.

Table 4: Gaussian fitting results for location errors with varied sampling frequency.

Sampling frequency (Hz)	Bimodal normal distribution				Unimodal normal distribution	
	Peak1		Peak2		Expectation	Variance
	Expectation	Variance	Expectation	Variance		
3000	-4.982	2.592	-2.011	4.735	-3.33956	3.09681
2500	-5.115	2.783	-1.515	4.74	-3.08597	3.31125
2000	-4.696	3.402	-0.9067	5.064	-2.83317	3.53732
1500	-4.814	3.511	-0.8707	5.473	-2.36894	3.87497

2.3.6. Location error in different direction

Micro-seismic monitoring systems for mining is not easy to deploy uniformly in three-dimensional space, elevation of different detectors is small gap. Detectors of monitoring system mainly distribute in an approximate plane space, which is in the X-Y plane. It leads inconsistent location error in different direction. In this section, location error distribution in different direction analyzed using the same simulation parameters. The P wave velocity is 2500 m/s, SNR is 7dB, quality factor is 10, sampling frequency is 2000 Hz, simulation duration time is 1s.

Location error in the Z direction is greater than location error in X and Y direction. In the Y direction, location error is less than in the X direction. Expectation and variance of bimodal/ Unimodal normal distribution in the Table 5 also indicated that location error in Z direction is much greater that other direction. Therefore, location result in Z direction is incredible.

Table 5: Gaussian fitting results for location errors in different direction.

Direction	Bimodal normal distribution				Unimodal normal distribution	
	Peak1		Peak2		Expectation	Variance
	Expectation	Variance	Expectation	Variance		
X	-1.729	5.058	5.126	3.206	-0.834907	4.08197
Y	-0.644	2.388	-0.6369	2.386	-1.14598	1.70317
Z	26.44	36.57	-27.77	43.6	-12.5392	36.8955

3. Borehole trajectory models

Borehole trajectory model can calculate trajectory coordinates using inclination and azimuth of borehole measuring point. According to assumptions for well trajectory, the mainstream calculation models of borehole trajectory are average angle method and minimum curvature method.

3.1. Average angle Method

Average angle method uses the average of the inclination and azimuth angles measured at the upper and lower ends of the survey section. The average of the two sets of angles is assumed to be the inclination and the direction for the course length. The well path is calculated with simple trigonometric functions[41].

Measurement points in the three-dimensional coordinate calculation method:

ISSN 2663-1563 Vol. 6, Issue 2: 51-64, DOI: 10.25236/AJAGE.2024.060210

$$X = \sum_{i=1}^{n} \Delta L_i \cos\left(\frac{\theta_i+\theta_{i+1}}{2}\right) cos\left(\frac{\alpha_i+\alpha_{i+1}}{2} - \lambda\right) \quad (14)$$

$$Y = \sum_{i=1}^{n} \Delta L_i \cos\left(\frac{\theta_i+\theta_{i+1}}{2}\right) sin\left(\frac{\alpha_i+\alpha_{i+1}}{2} - \lambda\right) \quad (15)$$

$$Z = \sum_{i=1}^{n} \Delta L_i \sin\left(\frac{\theta_i+\theta_{i+1}}{2}\right) \quad (16)$$

Where θ_i and θ_{i+1} is the inclination of upper and lower measurement points of course length, α_i and α_{i+1} is the azimuth of upper and lower measurement points, ΔL_i is the distance between upper and lower measuring points.

3.2. Minimum Curvature Method

The difference between the average angle method and minimum-curvature methods is that average angle method assume wellbore between upper and lower measure points is a straight line, whereas the minimum-curvature method assume wellbore between upper and lower measure points is a space arc and the tangential vector is in the same direction at the measuring point[41].

Measurement points in the three-dimensional coordinate calculation method:

$$\Delta X = K \frac{\Delta L}{2} (sin\theta_i cos\alpha_i + sin\theta_{i+1} cos\alpha_{i+1}) \quad (17)$$

$$\Delta Y = K \frac{\Delta L}{2} (sin\theta_i sin\alpha_i + sin\theta_{i+1} sin\alpha_{i+1}) \quad (18)$$

$$\Delta Z = K \frac{\Delta L}{2} (cos\theta_i + cos\theta_{i+1}) \quad (19)$$

$$K = \Delta L \frac{tan(0.5\varepsilon)}{\varepsilon} \quad (20)$$

$$cos\varepsilon = cos\theta_i cos\theta_{i+1} + sin\theta_i sin\theta_{i+1} \cos(\alpha_{i+1} - \alpha_i) \quad (21)$$

Where ΔX increment of the lower point of measurement relative to the upper point of measurement in north direction, ΔY increment of the lower point of measurement relative to the upper point of measurement in west direction, ΔZ increment of the lower point of measurement relative to the upper point of measurement in gravity direction, ε is angle between the upper measurement point tangent direction and the lower measurement point tangent direction[41].

3.3. Location error analysis

3.3.1. Simulated well trajectory

In this section, simulated well trajectory and survey data are proposed. The total length of simulation hole is 510m. The length of horizontal straight wellbore is 300m, the length of curved well hole is 210m. The curvature radius of a curved well hole is 210m. Interval of trajectory survey points is 3m. The wellbore is in the vertical and horizontal plane respectively, as shown in the Figure 5. This type of wellbore trajectory is mainly used for roof and floor drilling hole for methane extraction [1].

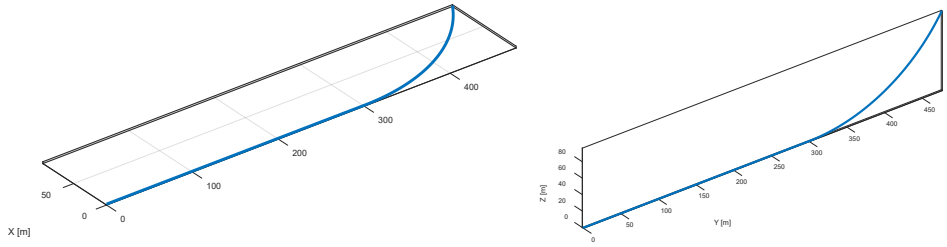

(a) The simulated well trajectory in the horizontal plane (Left)
(b) The simulated well trajectory in the vertical plane (Right)

Figure 5: The simulated well trajectory for roof and floor drilling hole

3.3.2. Location error analysis

Survey data of simulation drilling hole are added noise that satisfy gaussian distribution. The variance of inclination and azimuth angles error are 0.2 rad2 respectively. Simulation times of error analysis are set to 10000 times.

ISSN 2663-1563 Vol. 6, Issue 2: 51-64, DOI: 10.25236/AJAGE.2024.060210

According to simulation and statistical analysis results in the Table 6, expectation of location error in the Y direction is the greatest comparing errors in the X and Z direction. Variance of hole bottom location error is the smallest. In the X and Z direction, expectation of hole bottom location is small, however, variance of location error is great than X and Z direction. Therefore, hole bottom location results in X and Z direction are more accurate than Y direction.

Table 6: Gaussian fitting results for location errors with two methods (horizontal plane)

Method	Direction	Bimodal normal distribution				Unimodal normal distribution	
		Peak1		Peak2		Expectation	Variance
		Expectation	Variance	Expectation	Variance		
Average angle Method	X	-1.917	10.12	-14.13	5.085	-1.98786	7.22857
	Y	-9.083	4.149	-5.363	2.814	-9.45077	2.69794
	Z	-0.1465	11.45	-12.64	2.567	-0.116497	7.84686
Minimum Curvature Method	X	-2.323	2.805	-2.429	10.47	-2.48324	7.18811
	Y	-12.44	3.745	-17.31	2.375	-12.6108	2.70982
	Z	0.1737	11.29	12.19	2.831	0.0494757	7.76891

Above simulation analyzes results of hole bottom location error is distributed in horizontal plane. In this section, hole bottom location error in vertical plane is analyzed. Simulation parameters are consisting with the study of the horizontal plane.

The distribution of hole bottom location error is consistent with the previous study of the horizontal plane. The greatest expectation of location error is occurred in the Y direction. The expectation of location errors in X and Z direction in vertical plane is less than location errors in the horizontal plane. Consistent with previous analysis in the horizontal plane, location results of hole bottom in X and Z direction are more accurate than Y direction.

According to hole bottom location error analysis in the Table 7, Average angle Method location error is less than Minimum Curvature Method in the X and Y direction. In the Z direction, Minimum Curvature Method is better than Average angle Method.

Table 7: Location error probability density distribution in different direction (vertical plane)

Method		Bimodal normal distribution				Unimodal normal distribution	
		Peak1		Peak2		Expectation	Variance
		Expectation	Variance	Expectation	Variance		
Average angle Method	X	-1.917	10.12	-14.13	5.085	-0.033551	7.28517
	Y	-9.083	4.149	-5.363	2.814	-9.4457	2.68683
	Z	-0.1465	11.45	-12.64	2.567	-0.89313	7.28533
Minimum Curvature Method	X	-0.7959	10.43	-8.819	3.152	-0.872996	7.25164
	Y	-12.75	3.795	-18.24	2.395	-12.8345	2.74123
	Z	0.008598	10.21	-6.273	2.654	-0.037728	7.10304

4. Joint location method

Sensor data fusion methods mainly include weight method, Kalman filter and D-S decision theory[42]. Kalman filtering and weighting method are mostly widely used in sensors data fusion. This article adopts Kalman filtering and weighting method to merge of micro seismic location information and borehole attitude information.

4.1. Kalman filtering

Kalman filtering is a classic sensor data fusion technique used in application areas such as location and autonomous control of vehicles. Because of its ability to extract useful information from noisy data and its small computational and memory requirements, it is widely used in many industrial application areas[42]. In this paper, we combine two type of hole bottom location methods, which are micro-seismic location and MWD data location. Each positioning method calculates the X, Y and Z coordinates.

This paper considers the problem of choosing the optimal parameters α and β in the estimator for fusing location results of micro-seismic location and MWD location from uncorrelated variables[42]. The first reasonable requirement is that if the location results of two methods are equal, fusing them

ISSN 2663-1563 Vol. 6, Issue 2: 51-64, DOI: 10.25236/AJAGE.2024.060210

should produce the same value. This implies that

$$\alpha + \beta = 1 \tag{22}$$

Therefore, the linear estimators of interest are of the form[42]

$$X_\alpha(x_1, x_2) = (1-\alpha)x_1 + \alpha x_2 \tag{23}$$

$$Y_\beta(y_1, y_2) = (1-\beta)y_1 + \beta y_2 \tag{24}$$

$$Z_\beta(z_1, z_2) = (1-\gamma)z_1 + \gamma z_2 \tag{25}$$

The $x_1, x_2, y_1, y_2, z_1, z_2$ are considered to be unbiased estimators of some quantity of interest, then $X_\alpha, Y_\beta, Z_\beta$ is an unbiased estimator for any value of α, β, γ. One reasonable definition is that the optimal value of α minimizes the variance of $X_\alpha, Y_\beta, Z_\beta$ since this will produce the highest-confidence fused estimates[42]. The variance of $X_\alpha, Y_\beta, Z_\beta$ can be determined

$$\sigma_X^2(\alpha) = (1-\alpha)^2\sigma_{x1}^2 + \alpha^2\sigma_{x2}^2 \tag{26}$$

$$\sigma_Y^2(\alpha) = (1-\beta)^2\sigma_{y1}^2 + \beta^2\sigma_{y2}^2 \tag{27}$$

$$\sigma_Z^2(\alpha) = (1-\gamma)^2\sigma_{z1}^2 + \gamma^2\sigma_{z2}^2 \tag{28}$$

This result can be proved by setting the derivative of $\sigma_X, \sigma_Y, \sigma_Z$with respect to α to zero and solving equation for α, β, γ[42].

$$\alpha = \frac{\sigma_{x1}^2}{\sigma_{x1}^2+\sigma_{x2}^2} \tag{29}$$

$$\beta = \frac{\sigma_{y1}^2}{\sigma_{y1}^2+\sigma_{y2}^2} \tag{30}$$

$$\gamma = \frac{\sigma_{z1}^2}{\sigma_{z1}^2+\sigma_{z2}^2} \tag{31}$$

In the literature, the optimal value of α, β, γ is called the Kalman gain K. Substituting K into the linear fusion model[42], we get the optimal linear estimator

$$X(x_1, x_2) = \frac{\sigma_{x2}^2}{\sigma_{x1}^2+\sigma_{x2}^2}x_1 + \frac{\sigma_{x1}^2}{\sigma_{x1}^2+\sigma_{x2}^2}x_2 \tag{32}$$

$$Y(y_1, y_2) = \frac{\sigma_{y2}^2}{\sigma_{y1}^2+\sigma_{y2}^2}y_1 + \frac{\sigma_{y1}^2}{\sigma_{y1}^2+\sigma_{y2}^2}y_2 \tag{33}$$

$$Z(z_1, z_2) = \frac{\sigma_{z2}^2}{\sigma_{z1}^2+\sigma_{z2}^2}z_1 + \frac{\sigma_{z1}^2}{\sigma_{z1}^2+\sigma_{z2}^2}z_2 \tag{34}$$

Based on above derived data fusion formula based on Kalman filter, this paper conduct 10000 times simulation to calculate hole bottom position using micro-seismic and MWD information. The variance of calculation errors in X, Y and Z direction are listed in the Table 8.

Table 8: Location error probability density distribution with Kalman method

Direction	Micro-seismic location	MWD data location	Kalman filter
X	3.4886	7.2155	3.1507
Y	1.3527	2.7168	1.2194
Z	32.8932	7.1656	7.0134

According to the error variance of the simulation results, the micro-seismic location method is more accuracy than traditional location methods. However, location error in elevation is greater than in horizontal plane. The main reason is that the elevation of micro-seismic detectors is small. It causes greater location error in the elevation. However, wellbore attitude location method has less error in the Y direction.

In the X and Z direction, it has the same level of error with the proposed data confusion method. After fusion of micro-seismic location and MWD data, location error of hole bottom position decreases sharply in the all direction. Location errors in Z direction mostly decrease. In the case of high signal-to-noise ratio situation, the location errors in three directions X, Y and Z of 500 m length drilling hole is less than 1m.

ISSN 2663-1563 Vol. 6, Issue 2: 51-64, DOI: 10.25236/AJAGE.2024.060210

4.2. Weighting method

Weighting method is another important sensor data fusion method. This method is similar to Kalman filter method. However, calculation methods of weight coefficient are different from Kalman filter method. The coefficients of weighting method are usually calculated by linear fitting using field data. The coordinate calculation formula after fusion is shown as follows:

$$X_\alpha(x_1, x_2) = p(1)x_1 + [1 - p(1)]x_2 \tag{35}$$

$$Y_\beta(y_1, y_2) = p(2)y_1 + [1 - p(2)]y_2 \tag{36}$$

$$Z_\beta(z_1, z_2) = p(3)z_1 + [1 - p(3)]z_2 \tag{37}$$

According real coordinate and calculation coordinate of hole bottom, we can obtain $p(1)$ $p(2)$ $p(3)$ using least square method. Fitting result of least square method contain primary coefficients and constant terms. The primary coefficients are preserved and constant terms are discarded. The fitting result are presented in the following table. The fitting coefficient of X Y Z direction are 0.8157 0.7999 0.0442 respectively.

Table 9: Location error probability density distribution with weight method

Direction	Micro-seismic location	Trajectory location	Kalman filter
X	3.4739	7.3650	2.9835
Y	1.3508	2.7207	1.1458
Z	32.5437	7.2142	7.2025

According to weighting method results in the Table 9, location error variance of weighting method is better than the Kalman filter. It indicates that weighting method has better location precision. However, this method needs location error prior knowledge.

4.3. Prospect and application

According to the above analysis results, the proposed hole bottom joint positioning method can reduce the location error within 1 meter under ideal conditions. This method can be used in the directional drilling situation of coal mines. The patent [43] proposed a method and system for predicting the trajectory of a coal mine gas borehole using data measured during drilling. This method adopts axial force measuring instrument and ultrasonic caliper measuring instrument to calculate the steering ability of bottom hole assembly (BHA). The measuring range of axial force measuring instrument is from 0kN to 35kN. Calibrate the instrument, instrument output voltage is 0.004mV when axial force is 0kN, output voltage is 0.05mV when axial force is 1.5kN, output voltage is 0.112mV when axial force is 3.5kN. The fitting formula is output voltage = 3.0865×10^{-2}* axial force + 0.0039, Full scale accuracy is better than ±0.1%. The test and analysis results indicate that the joint location and trajectory control method can reduce the trajectory control error below ±1m under ideal situation. The research results of this paper can support the trajectory technology of extraction hole in coal mine.

5. Conclusion

This paper proposed a micro-seismic propagation model in the coal seam in mining area and hole bottom location method. Using established mode and proposed method, expectation and variance of location error in the all direction is analyzed. Micro-seismic location method has high precision in horizontal direction. However, location error in the vertical direction is great.

This paper also analyzes two types of widely used trajectory calculation methods, which are Average Angle Method and Minimum Curvature Method. According to expectation and variance of location errors, the Average Angle Method has higher accuracy than Minimum Curvature Method. In X and Z direction, two used location methods of hole bottom have the same level of location error. However, in the Y direction, location error is less than the other direction.

In this paper, two data fusion localization methods are proposed, which are Kalman method and weighting method. The Kalman filter method are based on the variance of the localization error to calculate weighting factor. The factor calculation of weighting method is based on difference between calculated and real hole bottom position. According to simulate results, the weighting method location are more accurate than Kalman filter method in the all direction.

ISSN 2663-1563 Vol. 6, Issue 2: 51-64, DOI: 10.25236/AJAGE.2024.060210

This paper proposed joint location method of coal mine methane extraction borehole trajectory using micro-seismic signal of rock breaking and MWD data. According simulate results, the proposed method can effectively improve the positioning accuracy of borehole bottom. The research results of this paper provide some theoretical reference for borehole positioning.

Acknowledgements

The Project has received support from the Key Research and Development Program of Sichuan Province, "Key Technologies for Autonomous Control of the Drainage borehole Drilling Trajectory of Coal Mines under Complex Geological Conditions" (2022YFG0244).

References

[1] Lou Z, Wang K, Kang M, et al. Plugging methods for underground gas extraction boreholes in coal seams: A review of processes, challenges and strategies [J]. Gas Science and Engineering, 2024, 122: 205225.
[2] Zheng C, Jiang B, Xue S, et al. Coalbed methane emissions and drainage methods in underground mining for mining safety and environmental benefits: A review [J]. Process Safety and Environmental Protection, 2019, 127:103-124.
[3] Yan B, Zhang X, Tang C, et al. A Random Forest-Based Method for Predicting Borehole Trajectories[J]. Mathematics, 2023, 11:1297-1311.
[4] Directional survey for 3D reservoir modelling [EB/OL]. https://petrowiki.spe.org/ Directional_ survey_for_3D_reservoir_modeling.
[5] Wei S, Liao X, Zhang H, et al. Recent Progress of Fluxgate Magnetic Sensors: Basic Research and Application[J]. Sensors, 2021, 21:1500-1518.
[6] Ningping Y, Jie Z, Xing J, et al. Status and Development of Directional Drilling Technology in Coal Mine[J]. Procedia Engineering, 2014, 73: 289-298.
[7] Qin M, Wang K, Pan K, et al. Analysis of signal characteristics from rock drilling based on vibration and acoustic sensor approaches[J]. Applied Acoustics, 2018, 140: 275-282.
[8] Wang X, Wang Q. Velocity estimating by optimizing micro-seismic observation system in complex terrain for underground illegal mining, Beijing, Virtual, China, 2021[C]. Aussino Academic Publishing House, 2021.
[9] Li N, Wang E, Ge M, et al. A nonlinear microseismic source location method based on Simplex method and its residual analysis [J]. Arabian Journal of Geoences, 2014, 7(11):4477-4486.
[10] Li N, Ge M, Wang E. Two types of multiple solutions for microseismic source location based on arrival-time-difference approach [J]. Natural Hazards, 2014, 73(2):829-847.
[11] Wang F, Xu G, Qu X, et al. Numerical simulation of microseismic wave propagation for underground gas storage: International Geophysical Conference, Qingdao, China, 17-20 April 2017, 2017[C].
[12] Giroux B. ttcrpy: A Python package for traveltime computation and raytracing [J]. SoftwareX, 2021, 16: 100834.
[13] Y. W, X. S, K. P. Relocating Mining Microseismic Earthquakes in a 3-D Velocity Model Using a Windowed Cross-Correlation Technique[J]. IEEE Access, 2020, 8: 37866-37878.
[14] Da Silva A A M, Novotny A A, Amad A A S, et al. Full-waveform reconstruction of micro-seismic events via topological derivative approach[J]. Journal of Computational Physics, 2024, 510: 113099.
[15] Wang F, Xu G, Qu X, et al. Numerical simulation of microseismic wave propagation for underground gas storage[C]. 2017 CGS/SEG International Geophysical Conference, Qingdao, China, 17-20 April 2017.
[16] Gomes V M, Santos M A C, Burgos R B, et al. Evaluation of the sensitivity of seismic inversion algorithms to different wavelets[J]. International Journal of Engineering Research and Applications, 2017, 06:59-73.
[17] Ciardelli C. Sensitivity kernels in seismic wave propagation: a simplified explanation for the banana-doughnut paradox[J]. European Journal of Physics, 2022, 43(4):45802.
[18] Julian B R, Gubbins D. Three-dimensional seismic ray tracing[J]. Journal of geophysics, 1977, 43:95-113.
[19] Karasözen E, Karasözen B. Earthquake location methods[J]. GEM - International Journal on Geomathematics, 2020,11(1):13.
[20] V I. Die berechnung der herdkoordinated eines nahbebens aus den dintrittszeiten der in einingen benachnbarten stationen aufgezeichneten P-oder P-wellen[J]. Gerlands Beitr Geophys, 1928,12(19):73-

ISSN 2663-1563 Vol. 6, Issue 2: 51-64, DOI: 10.25236/AJAGE.2024.060210

98.
[21] Thurber C H. Nonlinear earthquake location; theory and examples[J]. Bulletin of the Seismological Society of America, 1985, 75(3):779-790.
[22] Tang G. A general method for determination of earthquake parameters by computer[J]. Acta Seismologica Sinica, 1979, 1(2):186-196.
[23] Sambridge M, Gallagher K. Earthquake hypocenter location using genetic algorithms[J]. Bulletin of the Seismological Society of America, 1993,83(5):1467-1491.
[24] Klein K, Neira J. Nelder-Mead Simplex Optimization Routine for Large-Scale Problems: A Distributed Memory Implementation[J]. Computational economics, 2014,43(4):447-461.
[25] Fan S S, Zahara E. A hybrid simplex search and particle swarm optimization for unconstrained optimization[J]. European Journal of Operational Research, 2007,181(2):527-548.
[26] Allen R. Automatic phase pickers: Their present use and future prospects[J]. Bulletin of the Seismological Society of America, 1982,72(6B):S225-S242.
[27] Sleeman R, Eck T V. Robust automatic P-phase picking: an on-line implementation in the analysis of broadband seismogram recordings[J]. Physics of the Earth and Planetary Interiors, 1999,113(1-4):265-275.
[28] Takanami T, Kitagawa G. Estimation of the arrival times of seismic waves by multivariate time series model[J]. Annals of the Institute of Statistical Mathematics, 1991,43(3):407-433.
[29] Shang X, Li X, Morales-Esteban A. Enhancing micro-seismic P-phase arrival picking: EMD-cosine function-based denoising with an application to the AIC picker[J]. Journal of Applied Geophysics, 2018:S1969159069.
[30] Kirbas I, Peker M. Signal detection based on empirical mode decomposition and Teager–Kaiser energy operator and its application to P and S wave arrival time detection in seismic signal analysis[J]. Neural computing & applications, 2017,28(10):3035-3045.
[31] Ait Laasri E H, Akhouayri E, Agliz D, et al. Automatic detection and picking of P-wave arrival in locally stationary noise using cross-correlation[J]. Digital signal processing, 2014, 26: 87-100.
[32] Gholamy S, Javaherian A, Ghods A. Automatic detection of interfering seismic wavelets using fractal methods[J]. Journal of Geophysics and Engineering, 2008, 5(3):338-347.
[33] Romero J E, Titos M, Bueno Á, et al. APASVO: A free software tool for automatic P-phase picking and event detection in seismic traces[J]. Computers & Geosciences, 2016, 90: 213-220.
[34] Karamzadeh N, Javan Doloei G, Reza A M. Automatic Earthquake Signal Onset Picking Based on the Continuous Wavelet Transform[J]. IEEE Transactions on Geoscience and Remote Sensing, 2013, 51(5):2666-2674.
[35] Dai H, Macbeth C. Automatic picking of seismic arrivals in local earthquake data using an artificial neural network[J]. Geophysical Journal of the Royal Astronomical Society, 2010, 120(3):758-774.
[36] Liu H, Sun Z, Yin N K. Earthquake Detection STA/LTA[EB/OL]. https://cuseistut. readthedocs. io/en/latest/sta_lta/index.html.
[37] Wang H, Li M, Shang X. Current developments on micro-seismic data processing[J]. Journal of Natural Gas Science and Engineering, 2016, 32: 521-537.
[38] He X, Wang T, Wang X, et al. Fatigue behavior of direct laser deposited Ti-6.5Al-2Zr-1Mo-1V titanium alloy and its life distribution model[J]. Chinese Journal of Aeronautics, 2018, 31(11):2124-2135.
[39] Zhu S, Zhou F, Kang J, et al. Laboratory characterization of coal P-wave velocity variation during adsorption of methane under tri-axial stress condition [J]. Fuel, 2020,272:117698.
[40] Li X, Shang X, Morales-Esteban A, et al. Identifying P phase arrival of weak events: The Akaike Information Criterion picking application based on the Empirical Mode Decomposition[J]. Computers & Geosciences, 2017, 100:57-66.
[41] Calculation methods for directional survey[EB/OL]. https://petrowiki.spe.org/Calculation_methods_for_directional_survey.
[42] Pei Y, Biswas S, Fussell D S, et al. An Elementary Introduction to Kalman Filtering [J]. Communications of the ACM, 2019, 62:122-133.
[43] Wang X, Yan L, Deng G, et al. Prediction method and system of coal mine gas borehole trajectory driven by measurement data while drilling: 2023.12.22.